PHYSICAL REVIEW B

SOLID STATE

THIRD SERIES, VOL. 3, NO. 7 1 APRIL 1971

Phonon Avalanche in Ce-Doped Lanthanum Magnesium Double Nitrate

W. B. Mims and D. R. Taylor*
Bell Telephone Laboratories, Murray Hill, New Jersey 07974
(Received 3 August 1970)

We have studied the phonon avalanche in Ce^{3+}-doped lanthanum magnesium double nitrate (LMN) by making observations on the spin system. A variety of experimental techniques involving pulsed microwaves and pulsed magnetic fields have been used. We have measured the phonon lifetime and made observations which are related to the form of the acoustic power spectrum generated by the avalanche. Consideration of the magnitudes involved suggests that a transition probability model is adequate to explain the results obtained with our LMN + Ce samples, and that the first half of the avalanche can be described by a function of the form $1-\tanh\alpha(t-t_{1/2})$, where $t_{1/2}$ is the time at which the magnetization has fallen by $\frac{1}{2}$. Deviations from this function in the tail of the avalanche are due to phonon decay and to cross relaxation. The form of the hole burnt out by the avalanche has been calculated on the transition-probability model and agrees well with observations. Brief discussion of the fully nonlinear case is given. This would only be applicable if the acoustic gain, the acoustic intensity, or T_2 were several times larger than the values which we have assumed here.

I. INTRODUCTION

Paramagnetic relaxation phenomena can be simply and directly studied by monitoring the return to Boltzmann equilibrium after the level populations have been disturbed by applying a pulse of microwave power. Studies of this kind have, however, often revealed deviations from the exponential recovery law which one derives by assuming each spin to relax independently of the others with a constant probability $1/T_1$. We are concerned here with a particularly striking anomaly which is observed: (a) when the initial disturbed state corresponds to an inverted spin population, (b) when relaxation takes place via the emission of energy into a narrow band of lattice modes (direct process), and (c) when this acoustic energy is emitted faster than it can be dissipated. Under these circumstances the acoustic field, like the electromagnetic field in masers and lasers, will stimulate further emission and will give rise to a "phonon avalanche." This in turn leads to a catastrophic collapse of the inverted-spin population.[1]

We have studied the phonon avalanche in Ce^{3+}-doped lanthanum magnesium double nitrate (LMN) by making observations on the spin system. A variety of experimental techniques involving pulsed microwaves and pulsed magnetic fields have been used and are described in Sec. II. In particular we

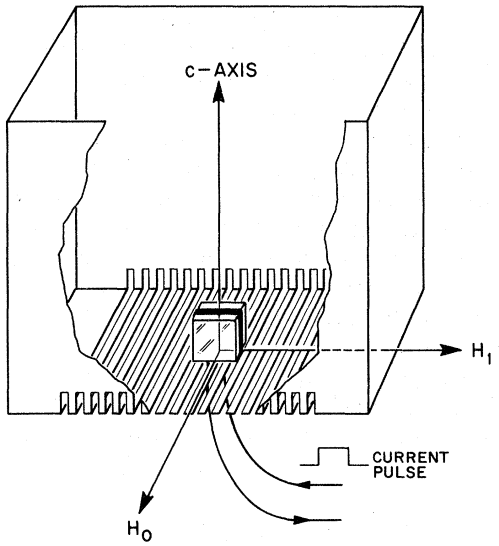

FIG. 1. TE_{100} cavity used in the phonon lifetime experiments. Slits were made in the wall so that induced currents would not impede the buildup and decay of the pulsed fields. The coil around the sample consisted of 5 turns of No. 38 wire.

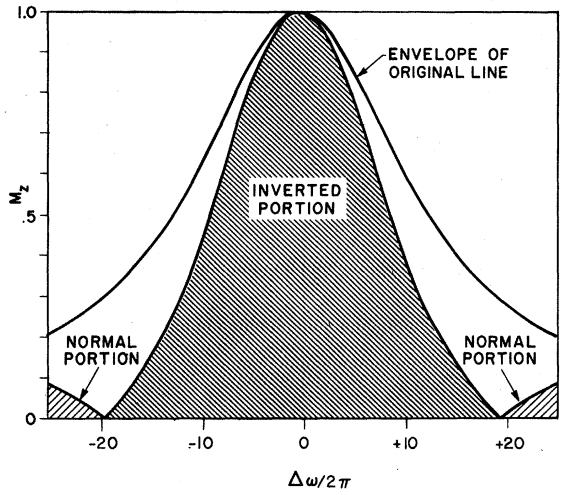

FIG. 2. Effect of applying a 180° pulse in a Lorentzian resonance line when the nutation frequency ω_1 is equal to the half-width at half-height $\Delta\omega_L$ of the line. The inverted portion is characterized by a half-width at half-height $\simeq 0.5\omega_1$. The horizontal scale is chosen to correspond to a line with $\Delta\omega_L/2\pi = 12.5$ MHz (i.e., a Ce, LMN line ~10 G full width at half-height).

have measured the phonon lifetime and have made some interesting experimental observations relating to the shape of the hole burnt out during the avalanche.

In Sec. III equations analogous to those commonly used to describe the growth of light waves in a laser are set up and applied to the problem of the growth of acoustic waves in the avalanche. It is shown that a pseudolinear approximation, equivalent to a transition-probability model of the avalanche, is almost certainly adequate to describe the interaction in the Ce LMN samples which we have studied. We have, however, briefly discussed the nonlinear case and indicated the conditions under which it could become important. The form of the avalanche hole, which at first suggests that the interaction is of the fully nonlinear type, can be satisfactorily explained in terms of the transition-probability model.

In Sec. IV we compare our results with those of Brya and Wagner[1] and attempt to account for the observed shape of the avalanche curve.

II. PULSE EXPERIMENTS

A. General

Microwave pulses at ~9.1 GHz were obtained from a 1-kW pulse traveling wave tube manufactured by Litton Industries. The tube was driven by a lower powered traveling wave tube which, in turn, was driven by a continuously running master oscillator klystron. Zeeman-field pulses of up to 60 G were obtained by passing currents of up to 10 A through four turns of 38 gauge wire wound around the samples[2] (see Fig. 1). The samples were ~3×3×2 mm in size.

In avalanche experiments the pulse sequence normally commenced with a 180° inverting pulse lasting for 20 nsec. This corresponds to a nutation rate $\omega_1 = \gamma H_1$ where[3] $\omega_1/2\pi = 25$ MHz. The full width at half-height of the resonance line was typically 25 MHz (10 G). Clearly therefore we have not been able to work under ideal 180° pulsing conditions for which ω_1 must considerably exceed the linewidth. This makes little difference to duration of the avalanche, however, although it does affect certain other properties as we shall indicate later. The effect of 180° pulse on a line whose half-width $\Delta\omega_L = \omega_1$ has been computed and is shown in Fig. 2.

Subsequent measurements on the recovering spin system were made, either by applying a 90° pulse in order to generate a free-induction signal, or by means of a two-pulse 120°-120° spin-echo sequence.[4] In the former case the largest available H_1, corresponding to $\omega_1/2\pi \sim 25$ MHz, was generally employed. Since the avalanche burns out a hole in the resonance line which is several times narrower than the line itself, e.g., ~10 MHz full width, this value of ω_1 is sufficient to generate an almost ideal free-induction signal from the spin packets concerned. In monitoring the depth of the burnt-out hole we used values of ω_1 several times smaller than those used to invert the line. Reduced values of H_1 were obtained by operating microwave switching diodes inserted between the klystron master oscillator and the traveling wave tubes. (Longer pulses were, of course, used when working with the reduced H_1.)

All measurements were made at 1.4 °K and with liquid helium in contact with the sample. The crystals were cut with a wet string and no attempt was made either to polish or to roughen surfaces in the experiments. As far as possible experiments were performed as soon as a new sample had been cut, and without repeated cycling to low temperatures. Some deterioration in the avalanche-generating property was noted in older and much used samples.

B. Experiments to Determine Phonon Lifetime in Sample

The sequence of events in these experiments is shown in Fig. 3. The initial experiment is made with no Zeeman-field pulse. Pulse I then inverts the spin system and pulses II and III generate a spin-echo signal which is proportional to the population difference in that part of the resonance line which is being observed.[5] If the time t between pulse I and pulse II is varied (while τ the time between pulses II and III is held constant) the echo amplitude traces out the course of the avalanche.

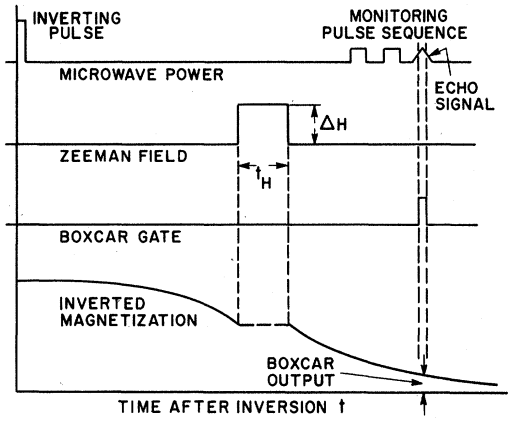

FIG. 3. Timing sequence for the phonon lifetime experiment.

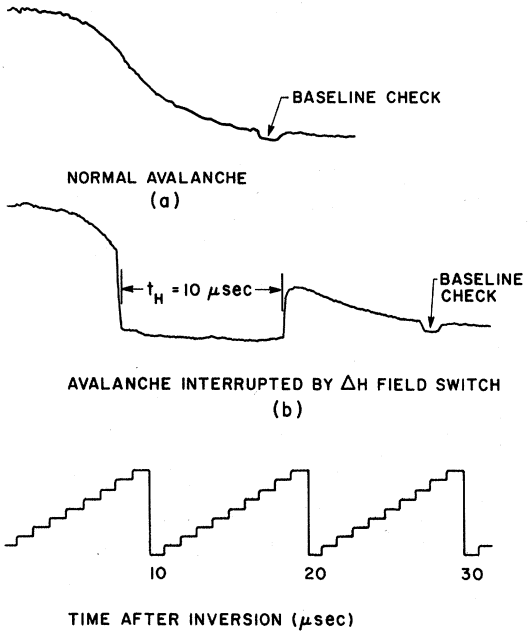

FIG. 4. Boxcar tracings showing the phonon avalanche with and without the Zeeman-field pulse. The staircase timing function was obtained from a HP 524B counter with time interval plug-in unit 526B.

A tracing made by boxcar methods is shown[6] in Fig. 4(a). Suppose now that we apply a Zeeman-field pulse for a time t_H between pulses I and II. At the beginning of the interval t_H resonance between the band of phonons which contains the avalanche acoustic energy and the driving spin system is abruptly broken, leaving the acoustic energy to decay on its own. At the end of t_H the residue of this energy is returned to the spins and the avalanche is allowed to continue[7] as shown in Fig. 4(b). The reduction in the avalanche rate can then be used as an approximate measure[8] of the decay of acoustic energy during the time t_H. By repeating this experiment for several values of t we were able to estimate the phonon lifetime in our samples. The results are shown in Table I.

It should perhaps be stressed that what we measure is not the lifetime of any specific phonon mode or set of modes. We do not know which modes are most strongly coupled with the Ce^{3+} spin system, nor do we know the probabilities for mode conversion in our sample. The measurement is in fact akin to the measurement of a "reverberation time" of a hall in classical acoustics. The chief significance of the result $t_{\text{phonon}} \sim 20$ μsec from our point of view lies in the fact that the phonon lifetime is appreciably longer than the time which characterizes the avalanche itself. It seems therefore that loss of acoustic energy can only play a minor role during the buildup of the avalanche. It may also be noted that the phonon lifetime is sufficient to

TABLE I. Experimental results.

Sample	Concentration (nominal) (%)	Linewidth (G)	Avalanche time[a] (μsec)	T_2 (μsec)	Inversion efficiency (%)	Phonon lifetime (μsec)	Spectral diffusion time[b] (μsec)
A	0.3	8	7.7	4	80	20±40%	130
B	0.5	12	7.8	4	88		80
C	0.5	13	9.5		89	20±20%	
D	0.8	12	1.7	0.84	65		12
E	1.3	25	~1.6[c]	0.32	44		1.6
F	2.0	38	No avalanche[d]	0.24	54		1.7

[a] Defined as the interval between inversion of the line and 50% collapse of the initial inverted magnetization.

[b] Time for initial $1/e$ fall of stimulated echo for $\tau = 150$ nsec. See text.

[c] Avalanche time is approximate because of rapid decay of the inverted magnetization due to spectral diffusion.

[d] Inverted magnetization was observed to collapse in a time ~2 μsec but this was apparently caused by spectral diffusion.

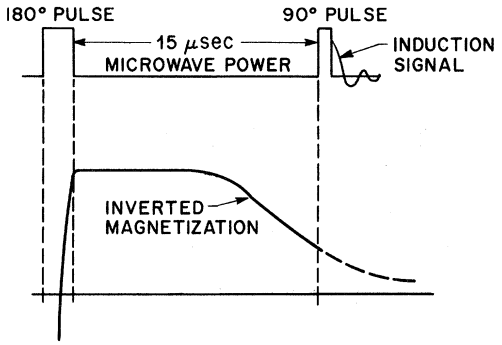

FIG. 5. Timing sequence used in experiments to find the shape of the hole burnt out by the avalanche.

allow for several complete traversals of the sample.[9] All resonant Ce^{3+} spins, whatever their location in the sample, will therefore be equally involved.

C. Form of Hole Burnt Out during Avalanche

So far we have implied that the hole burnt out by the avalanche has a more or less smooth and regular form similar to, though narrower than the resonance line itself. Pulse methods enable us to investigate the burnt-out hole shape in some detail and reveal certain surprising and unexpected features. For the experimental pulse sequence we refer to Fig. 5. Pulse I is as before a 180° inverting pulse; pulse II is a 90° pulse applied at a selected stage in the development of the avalanche. It is easily shown that, for an inhomogeneous line, the free-induction signal generated by a 90° pulse is the Fourier transform of the line shape. Since our line shape can be regarded as a superposition of the original inverted line shape (Fig. 2) and the hole burnt out by the avalanche we expect the free-induction signal to be given by the sum of the two appropriate Fourier transforms. The first transform, that of the initial line shape, will be characterized by a decay time $\simeq 10$ nsec and will be masked by cavity ringing and other overload effects in the apparatus. The second transform (or at least the latter part of it) is visible as a free-induction trace.

Figure 6 shows free-induction signals obtained by combining several oscilloscope photographs at different gain settings.[10] In Figs. 6(a) and 6(b) the maximum available H_1 ($\gamma H_1/2\pi \sim 20$ MHz) was used in the 180° pulse in order to invert as much of the line as possible. Figure 6(a) shows the free-induction trace obtained by applying the 90° pulse 6 μsec after the inverting pulse, i.e., at a point about $\frac{1}{3}$ way down the avalanche. In Fig. 6(b) the 90° pulse was applied 20 μsec after the inverting pulse, i.e., when the avalanche was virtually over. Generally, the effect of applying the 90° pulse later was to in-

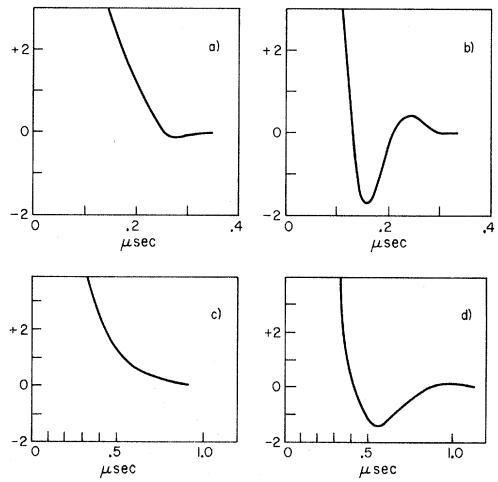

FIG. 6. Free-induction signals arising from the hole burnt out in the resoance line by the avalanche in a 0.5% sample: (a) was obtained by applying the 90° pulse 6 μsec after the inverting pulse, at which time the magnetization had fallen by $\frac{1}{3}$; (b) was obtained by applying the 90° pulse 20 μsec after the inverting pulse, i.e., at the end of the avalanche; (c) and (d) show the results of a similar experiment in which H_1, and therefore the spectrum of spin packets inverted during the 180° pulse was ~8× smaller.

crease the amplitude and, to a slight extent, to shorten the period of the oscillatory feature which appears in the tail of the free-induction signal. If times $\gtrsim 20$ μsec were allowed to elapse after the end of the avalanche before applying the 90° pulse the induction signal was weaker, presumably because of the filling in of the burnt-out hole by cross relaxation.

The experiments were repeated with reduced values of H_1 in the inverting pulse so that the effect

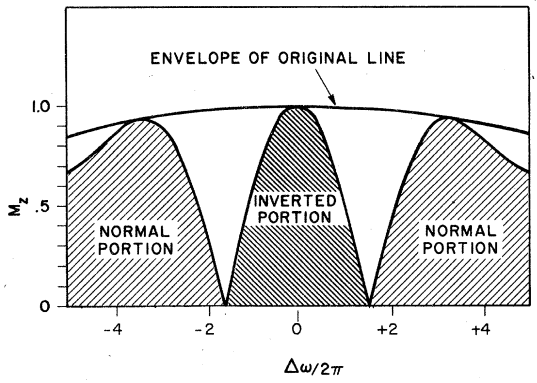

FIG. 7. Portion of a resonance line which is inverted by a 180° pulse if $\omega_1 \ll$ linewidth. Here $\omega_1 \sim 12\times$ less than the half-width of the resonance line. The horizontal scale is chosen to correspond to the application of a 180° pulse 250 nsec long.

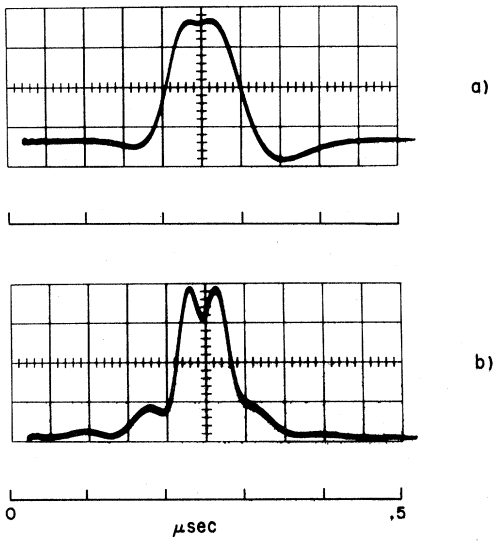

FIG. 8. Spin-echo signals generated from a resonance line partially burnt out by an avalanche. Concentration = 0.5%. Two echo generating pulses each 25 nsec long applied (a) 6 μsec, (b) 20 μsec after a 30-nsec inverting pulse. Values of H_1 used to generate echoes were the same as the values of H_1 used in the inverting pulses, and not reduced as in the phonon lifetime experiments.

of inverting narrower spectral intervals could be studied. (When $\omega_1 \ll$ linewidth a 180° pulse inverts a portion of the line such that its half-width at half-height $\simeq 0.5\omega_1$, see Fig. 7.) Figures 6(c) and 6(d) show the result of one such test in which $\gamma H_1/2\pi \sim 2.5$ MHz. In Figs. 6(c) and 6(d) the 90° pulses were once again applied at 6 and 20 μsec after the inverting pulse. Exact comparisons are hard to make, but it would appear from Figs. 6(b) and 6(d) that the free-induction signal is ~4 times longer in this latter case, and correspond to the burn out of a hole which is similar in shape but ~4 times narrower. Some further tests were made to try and ascertain how far H_1 could be reduced without causing these effects to disappear entirely. It was observed that the free-induction signal (due to the hole burnt in the line) underwent a drastic reduction when $\omega_1/2\pi$ was reduced below ~1.5 MHz. We believe this to be due to the filling in of the hole by cross relaxation as fast as it is burnt out by the avalanche.[11]

As we mentioned at the beginning of Sec. II C, overload effects made it impossible to observe the initial portion of the free-induction trace. Since the echo signal is, ideally, given by two free-induction signals back to back, the effects should therefore be more clearly visible in the spin-echo signal. Although in practice this turned out to be an inconvenient way of studying the shape of the hole – largely because of the short phase memory times – we show here two echo photographs obtained at different stages in the avalanche in a 0.5% sample. The echo in Fig. 8(a) was obtained by applying two microwave pulses 6 μsec after the inverting pulse. In Fig. 8(b) an interval of 20 μsec was allowed to elapse. The echoes show the same oscillatory feature observed in the free-induction signal. It should be noted that these echoes were generated by applying large microwave fields H_1 and not reduced fields as when sampling the center of the avalanche hole. The reduced fields, as used, for example, in the phonon lifetime experiments, generated echo signals of longer duration and with more regular form.

We were interested in finding out to what extent the traces in Fig. 6 betray the nature of the acoustic fields as they exist in the fully developed avalanche. The traces themselves are, of course, the cumulative result of the spin-phonon interaction throughout the avalanche from its inception onwards. We were able to make a separate test of this point as follows: A modified experiment was performed by applying a Zeeman-field shift and replacing the spins which had generated the avalanche with spins from the wings of the Ce^{3+} line. The acoustic field then burnt a new hole leaving its imprint on these new unused spins. The new hole was examined, as before, by applying a 90° pulse and observing the free-induction decay. This modified procedure[12] gave essentially the same induction signals as those[13] in Fig. 6. For practical purposes we may therefore assume that the periodicity seen in the free-induction signal in the straightforward 180°-90° pulse experiment arises primarily from interaction with the more intense acoustic fields which are generated in the mature avalanche.

D. Measurement of T_2

T_2 was measured by means of a two-pulse spin-echo sequence. The results are given in Table I. They represent an estimate of the time measured from pulse I of the sequence, in which the echo signal falls to $1/e$ of its maximum value. The time was not easy to determine accurately since (a) the echo envelope was not exponential and (b) the result was liable to be modified by "instant diffusion"[14] effects. Nonexponentiality of the envelope (further complicated here by modulation at the N^{14} nuclear precession frequencies) was probably only a minor source of error.[15] Instant diffusion, on the other hand, led to values of T_2 several times too short unless suitable precautions were taken. The shortening of the apparent phase memory occurs as a result of the abrupt change in local dipolar fields which occur when the spins are inverted by the second pulse of the two-pulse sequence. The effect can be reduced by turning over smaller fractions of the resonance line, either by using

a small H_1 (and longer pulses), or by making the measurement in the wings of the line. In this way a limiting value for T_2 can be obtained. This procedure does not necessarily give a value of T_2 which accurately describes the dynamical behavior of the spin packets during the avalanche, since the avalanche itself changes local fields and introduces instant diffusion. We are, however, primarily interested here in obtaining the correct order of magnitude. As may be seen by comparing Fig. 4(a) and the times in Table I, T_2 is comparable with the time taken by the magnetization to collapse during the avalanche.

E. Test for Spin-Phonon Coherence

The resonant transfer of energy from a precessing spin system to an acoustic wave will be characterized by some degree of coherence, although this may well be masked in the bulk of the sample by the occurrence of many independent regions in which this transfer is taking place. We shall argue later (Sec. III B) that in the more dilute samples, this coherence time is effectively equal to the autocorrelation time of the acoustic field generated in the avalanche, and that it is an order of magnitude shorter than the spin-echo phase memory time. In order to confirm this point experimentally we performed the following test aimed at setting a lower limit on the spin-phonon coherence time.

The system was set up as in Sec. II A for the observation of the avalanche. At a chosen time after pulse I a small displacement ΔH was made in the Zeeman field by applying a current pulse to the coil surrounding the sample. The current pulse was maintained for a time Δt such that[16] $\gamma \Delta H \Delta t = 180°$. By reversing the phase of the spin system such a pulse should arrest growth of the avalanche (or avalanches if several regions of the sample are involved) for a time comparable with the coherence time of the interacting systems. Under no circumstances were we able to observe any effects. Since an extension of the time required for full development of the avalanche by 0.5 μsec would have been clearly visible, we conclude that any coherence times are shorter than this.

F. Change of Samples, Half-Fall Times, Concentration Effects

We have examined a number of different samples, partly as a check on our principal observations, and partly in order to see how they depend on spin concentration. Some of the results of these experiments are shown in Table I. The characteristically shaped avalanche curve was obtained for all but the 2% sample. In this sample the portion of the line inverted by the 180° pulse was considerably smaller than the total linewidth and collapsed rapidly because of spectral diffusion from the remaining uninverted portions of the line. If was impossible to judge from the shape of the decay curve whether or not a phonon avalanche was contributing to this collapse.[17] A free-induction signal with a periodic tail, arising as a result of the avalanche (Sec. II C), was seen in all but the 2% sample. This again does not prove conclusively that no avalanche occurred, since rapid spectral diffusion would also be likely to blur out any sharp features in the avalanche hole. The phonon lifetime was checked in the two weaker samples. Shortening of the phase memory and of the avalanche time made it difficult to execute all the steps involved in this experiment at the higher concentrations. The spin-phonon coherence time experiment (Sec. II E) was performed only once – with a 0.5% sample.

If we make the transition-probability approximation and introduce the experimentally observed fact that the phonon lifetime is longer than the total avalanche time, we find (Sec. III B) that the decay of the initial inverted magnetization should roughly follow the curve

$$M_{z,\omega} = (\tfrac{1}{2} M_{z,\omega,0})[1 - \tanh \alpha_{t,\omega}(t - t_{1/2,\omega})] \ , \qquad (2.1)$$

where $M_{z,\omega}$ is the magnetization, $2\alpha_{t,\omega}$ is the initial phonon power gain constant (before burn out), and $t_{1/2,\omega}$ is the time at which $M_{z,\omega}$ has collapsed halfway. $M_{z,\omega}$, $\alpha_{t,\omega}$, and $t_{1/2,\omega}$ refer to a specific spectral position in the inhomogeneous line. In most experiments this is the center of the line and we shall drop the subscript ω wherever there is no likelihood of ambiguity. Equation (2.1) will become inaccurate in the tail of the avalanche, where phonon decay and cross relaxation play a relatively larger role (Sec. IV B). It will be good enough, however, to provide a relationship between $2\alpha_t$ and the time interval $T_{1/2}$ which elapses between the inverting pulse and $t_{1/2}$. If S is the ratio of the total available avalanche energy (primarily spin energy) to the initial acoustic energy, it is shown in Sec. III B [Eq. (3.24)] that

$$T_{1/2} = (1/2\alpha_t) \ln S. \qquad (2.2)$$

$T_{1/2}$ will depend on $N_{z,\omega,0}$, the initial excess of inverted spins/cm^3 per unit spectral interval, both via α_t and via S. α_t is directly proportional to $N_{z,\omega,0}$. S is directly proportional to $N_{z,\omega,0}$, provided that comparisons are made between samples at the same initial lattice temperature.[18]

For rough comparisons between samples we may ignore variations in S (which is $\simeq 10^4$) and merely take $T_{1/2}$ as a measure of the gain constant $2\alpha_t$. In a series of experiments performed at the same temperature T we should then expect to find that $1/T_{1/2}$ is proportional to the product of the concentration and the inversion efficiency divided by the linewidth. The agreement with this prediction is very poor as may be verified by glancing at Table I.

We do not fully understand the reasons for this. At the 1.3% concentration $T_{1/2}$ was probably shortened by spectral diffusion effects which deformed the avalanche curve. The remaining results hardly show any better agreement, however. Some discrepancies may have been due to the difficulty of measuring the inversion efficiency by spin echoes when the avalanche time is of the order of the time required for the two-pulse sampling sequence.[19] Others may have arisen in the linewidth measurements, which showed a disturbing tendency to change in successive low-temperature runs.[20]

In view of our lack of success in confirming a proportionality between $1/T_{1/2}$ and $N_{z,\omega,0}$ by comparing different samples we have studied the relationship by using the microwave pulsing conditions to vary $N_{z,\omega,0}$. This can be attempted in two ways. The simplest is to apply a pulse inducing a spin nutation angle of less than 180°. An alternative method is to increase the recurrence rate of the pulsing cycle so that the spin system is partially saturated at the beginning of each experiment. Both of these procedures are open to some objections, in particular the latter which may result in some heating of the lattice phonons,[21] but both have in practice given fairly good results. Curves of $1/T_{1/2}$ plotted against the initial value of $N_{z,\omega}$ (see, for example, Fig. 9) have shown a reasonable degree of linearity. Deviations at long values of $T_{1/2}$ are easily explained by the increased importance of spectral diffusion and phonon decay in this limit.

Spectral diffusion, although clearly responsible for influencing a number of observations, proved difficult to parametrize (see Ref. 11), and we eventually abandoned the attempt to employ it to give quantitative interpretations of the results. We have, however, retained a small sampling of our spectral diffusion measurements and included them in Table I. These were obtained in a series of stimulated echo experiments. They are the e-fall times as a function of the time T between pulses II and III, when the time τ between pulses I and II was set at 150 nsec. They give a rough measure of the time taken for a spin packet to spread out into a distribution ~2 MHz wide. The times required for diffusion to spread across wider intervals may be gauged from the graphs in Fig. 16 which trace the filling in of holes burnt in the resonance line in a 0.5% sample.

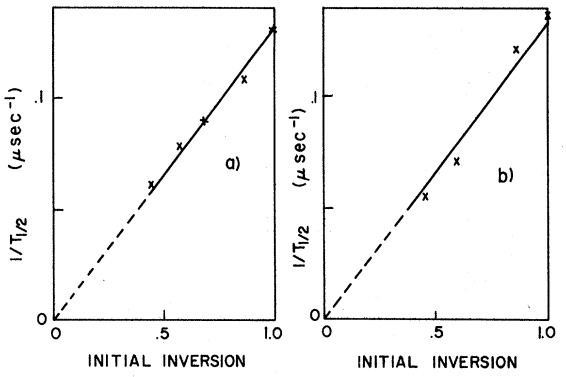

FIG. 9. Reciprocal of avalanche half-fall time $T_{1/2}$ plotted as a function of the initial population inversion for a 0.5% sample. (Maximum experimental inverted signal, shown here as unity, was ~0.85 of the uninverted signal amplitude.) (a) Inversion reduced by applying < 180° inverting pulse; (b) inversion reduced by operating with a pulse recurrence rate causing partial spin saturation.

III. THEORY

A. Interaction of Acoustic Waves with a Two-Level System

The buildup of a phonon avalanche in a paramagnetic material may be expected in some ways to resemble the growth of an electromagnetic wave in a laser crystal. Numerous discussions of the latter problem have appeated in the literature.[22-27] We shall therefore attempt to formulate the avalanche problem in a parallel manner. This will facilitate comparison with the laser work, and will enable us to discuss the possibility of nonlinearity in the spin-phonon interaction. In making this formulation, we shall, wherever possible, adapt concepts which are already familiar in the field of magnetic resonance.

We first parametrize the interaction between spins and acoustic waves. For the case of a Kramers doublet this interaction is commonly specified by adding a term

$$\mathcal{H}_{SL} = \mu_B G_{ijkl} e_{kl} H_i S_j \qquad (i,j,k,l = 1,2,3) \qquad (3.1)$$

to the spin Hamiltonian. G_{ijkl} is a fourth-rank "magnetoelastic" tensor, e_{kl} is the strain tensor, and H_i are components of the Zeeman field $\vec{H}_0$. $\mathcal{H}_{SL}$ induces transitions between the eigenstates of the unperturbed Hamiltonian $\mathcal{H}_0 = \mu_B g_{ij} H_i S_j$. Since we are concerned with experiments performed with $\vec{H}_0 \perp$ the c axis in an axial material we can at once reduce the number of indices in Eq. (3.1). We take the z axis ($i = 3$) parallel to $\vec{H}_0$. Then S_z is a good quantum number and transitions are induced solely by $S_x (= S_1)$ and $S_y (= S_2)$, leaving

$$\mathcal{H}_{SL} = \mu_B H_0 (G_{31kl} S_x + G_{32kl} S_y) e_{kl} \quad . \qquad (3.2)$$

At this point we make some additional arbitrary simplifications. We assume (a) that the medium is acoustically isotropic and (b) that all the independent parameters in G_{ijkl} have the same numerical value G', and (c) we ignore interactions with longitudinal waves. It is then sufficient to

consider the interaction of the spin system with a single (linearly polarized) transverse wave characterized by an oscillating strain

$$s_T = 2s\cos[\omega t - (\omega/v)\zeta - \psi]$$
$$= s(e^{i[\psi-\omega t+(\omega/v)\zeta]} + e^{-i[\psi-\omega t+(\omega/v)\zeta]}) \quad , \qquad (3.3)$$

in which ζ is the distance measured along the direction of propagation of the wave.[28] In a system of spin coordinates rotating about the z axis with a phase factor $e^{i[\psi-\omega t+(\omega/v)\zeta]}$ this strain is represented by a vector of length s lying along the x axis. (The strain $s\,e^{-i[\psi-\omega t+(\omega/v)\zeta]}$ will not induce transitions.) The Hamiltonian in this system becomes $\mathcal{H}'_{SL} = G'\mu_B H_0 s(S_x + S_y)$ and can readily be reduced by a further rotation of the spin axis to give

$$\mathcal{H}''_{SL} = G\mu_B H_0 s S'_x \quad , \qquad (3.4)$$

where $G = \sqrt{2}\,G'$. An appropriate value for the coupling parameter G can be obtained from the direct process lattice relaxation time T_{1d}. If we derive T_{1d} from $\mathcal{H}_{SL}$, allowing for two transverse waves, but ignoring the longitudinal component, we find that

$$\frac{1}{T_{1d}} = \frac{(G\mu_B H_0)^2 kT\omega_0^2}{2\pi\hbar^2 v^5 \rho} \quad , \qquad (3.5)$$

where v is the transverse sound velocity, ρ is the density, and ω_0 is the paramagnetic resonance frequency.

By comparing (3.4) with the familiar Hamiltonian $\mathcal{H}'_{rf} = g\mu_B H_1 S_x$, which would describe the interaction of a spin system (of isotropic g) with a linearly polarized rf field $H_x = 2H_1\cos[\omega t - (\omega/v)\zeta - \psi]$, we can at once infer the strain-induced nutation rate. In the rotating coordinate system adopted here H_x would be represented by a vector $\vec{H}_1$ lying along the x axis and the nutation frequency would be given by $\omega_{rf} = \gamma H_1$ where $\gamma = g\mu_B/\hbar$. Instead of H_x we have a linearly polarized strain wave $s_T = 2s\cos[\omega t - (\omega/v)\zeta - \psi]$, and a Hamiltonian $\mathcal{H}''_{SL} = G\mu_B H_0 s S_x$. The nutation frequency is therefore $\omega_s = \Gamma_s$, where

$$\Gamma = G\mu_B H_0/\hbar \quad . \qquad (3.6)$$

The over-all changes associated with nutation and precession can be defined quantum mechanically in terms of the density matrix

$$\rho = \begin{bmatrix} \rho_{11} & \rho_{12} \\ \rho_{12}^* & \rho_{22} \end{bmatrix}$$

and described macroscopically by means of the Bloch equations:

$$\frac{\partial N_x}{\partial t} = \left(\Delta\omega + \frac{\partial\psi}{\partial t}\right)N_y - \frac{N_x}{T_2'} \quad , \qquad (3.7a)$$

$$\frac{\partial N_y}{\partial t} = -\left(\Delta\omega + \frac{\partial\psi}{\partial t}\right)N_x - \frac{N_y}{T_2'} - \Gamma s N_z \quad , \qquad (3.7b)$$

$$\frac{\partial N_z}{\partial t} = \Gamma s N_y \quad . \qquad (3.7c)$$

The following points should be noted in connection with Eq. (3.7):

(a) The T_1 term has been omitted in (3.7c) since T_1 is several orders of magnitude longer than any times which concern us here. Enhanced relaxation due to the avalanche is, of course, taken into account in the terms $\Gamma s N_z$ and $\Gamma s N_y$.

(b) The spins precess in the rotating system with a frequency $\Delta\omega + \partial\psi/\partial t$, where $\Delta\omega$ is the difference between ω and the Larmor frequency of a given spin packet. The term $\partial\psi/\partial t$ is an additional frequency representing gradual changes in the phase ψ of the acoustic wave which here determines the rotation $e^{i[\psi-\omega t+(\omega/v)\zeta]}$ of the coordinate system. In the laboratory system the coordinate axes rotate at any given instant with a frequency $\omega - \partial\psi/\partial t$.

(c) The loss of coherence of the spin system in relation to the rotating coordinate axes used in (3.7) is not determined by random perturbations of the spin system only. If the spins are driven by a noise field, as here, an additional random element will appear due to fluctuations in the phase angle ψ of the coordinate system. It is convenient to combine both these effects in a single decay constant T_2'. (T_2' is used instead of T_2 to emphasize the difference between the present case and the more usual case where the field driving the spin system is monochromatic.)

(d) The quantities N_j are defined from the density matrix by $N_j = \frac{1}{2}N\,\mathrm{Tr}(\rho\sigma_j)$, where N is the total number of spins/cm^3 (or, where appropriate, the total number of spins/cm^3 belonging to any given spin packet), and the σ_j are the Pauli spin matrices. We thus have $N_x = N(\rho_{12} + \rho_{12}^*)$, $N_y = iN(\rho_{12} - \rho_{12}^*)$, $N_z = N(\rho_{11} - \rho_{22})$. N_x, N_y, and N_z can be regarded as components of a precessing vector $\vec{N}$. N_z is the excess number of spins/cm^3 in the upper state. For the case of an isotropic g the Bloch equations could equally well have been written in the more familiar form in which the magnetization components $M_j = g\mu_B N_j$ take the place of the N_j. Here, however, the field does not interact with M_j and we are concerned instead with the stresses $P_j = G'\mu_B H_0 N_j$ which result from spin precession. In the laboratory system $P_1 = P_x$ and $P_2 = P_y$ are oscillating stresses in phase and in quadrature with the strain, the linearly polarized traveling stress wave being given by

$$P_{lab} = \mathrm{Re}[(P_x + iP_y)\,e^{i[\psi-\omega t+(\omega/v)\zeta]}] \quad .$$

The component $P_3 = P_z$ is a small static stress which can be ignored.

We now consider the effect of these oscillating stresses on the growth of a plane acoustic wave. If we introduce P_{lab} when deriving the differential equation for an elastic wave traveling in the ζ direction in an isotropic medium we obtain

$$\frac{\partial^2\epsilon}{\partial\zeta^2}=\frac{1}{v^2}\frac{\partial^2\epsilon}{\partial t^2}=\left(\frac{1}{\rho v^2}\right)\frac{\partial^2(p_{lab})}{\partial\zeta^2} \quad , \tag{3.8}$$

where ϵ is the strain, $v^2=q/\rho$, and q is the elastic constant. Substituting $\epsilon=2s\cos[\omega t-\psi-(\omega/v)\zeta]$, and assuming that we are dealing with a more or less monochromatic acoustic wave, whose phase ψ and strain amplitude s change slowly over one wavelength (or cycle), we can derive from (3.8) the two first-order equations[29]

$$\frac{\partial s}{\partial\zeta}+\frac{1}{v}\frac{\partial s}{\partial t}=-\frac{\omega P_y}{4\rho v^3}=-aN_y \quad , \tag{3.9a}$$

$$s\frac{\partial\psi}{\partial\zeta}+\frac{1}{v}\frac{\partial\psi}{\partial t}=+\frac{\omega P_x}{4\rho v^3}=+aN_x \quad , \tag{3.9b}$$

where

$$a=\frac{G'\mu_B H_0\omega}{4\rho v^3}=\frac{G\mu_B H_0\omega}{4\sqrt{2}\,\rho v^3} \quad . \tag{3.9c}$$

The expressions $\partial s/\partial\zeta+(1/v)\,\partial s/\partial t$ and $\partial\psi/\partial\zeta+(1/v)\,\partial\psi/\partial t$ give the rates of change of s and ψ from the point of view of an observer traveling with the wave. These two equations together with the Bloch equations (3.7) describe the mutual interactions of the spins and the traveling wave.

B. "Transition-Probability" Approximation

In the initial states of the avalanche s will be small, N_x, N_y will be $\ll N_z$, and N_z itself will be scarcely affected by the acoustic interaction. In this regime the medium constitutes a linear amplifier for the acoustic waves. Even outside this regime, when the avalanche has continued long enough to cause significant burn out of N_z, a pseudosteady state may exist in which the medium acts as a linear amplifier, although here it will be an amplifier of steadily diminishing gain. Linear gain of this type occurs if s, $\partial\psi/\partial t$, and N_z diminish by relatively small amounts during the time T_2' [as can be shown by making an approximate integration of (3.7a) and 3.7b)]. The essential condition is that

$$\Gamma s T_2'\ll 1 \quad . \tag{3.10}$$

If this condition is met, N_x, $N_y\ll N_z$ and are given by

$$N_x=\frac{\Gamma s N_z(T_2')^2(\Delta\omega+\partial\psi/\partial t)}{1+(T_2')^2(\Delta\omega+\partial\psi/\partial t)^2} \quad ,$$

$$N_y=\frac{\Gamma s N_z T_2'}{1+(T_2')^2(\Delta\omega+\partial\psi/\partial t)^2} \quad . \tag{3.11}$$

Inserting the values (3.11) in the traveling wave Eqs. (3.9a) and (3.9b) we find that the growth in amplitude and the phase change of the wave as it travels forward in the medium are given by

$$\frac{ds}{d\zeta}=\left(\frac{\partial s}{\partial\zeta}+\frac{1}{t}\frac{\partial s}{\partial t}\right)=\frac{a\Gamma T_2' N_z s}{1+(T_2')^2(\Delta\omega+\partial\psi/\partial t)^2} \tag{3.12}$$

and

$$\frac{d\psi}{d\zeta}=\left(\frac{\partial\psi}{\partial\zeta}+\frac{1}{v}\frac{\partial\psi}{\partial t}\right)=-\frac{a\Gamma(T_2')^2 N_z(\Delta\omega+\partial\psi/\partial t)}{1+(T_2')^2(\Delta\omega+\partial\psi/\partial t)^2} \quad . \tag{3.13}$$

For a *homogeneous* line the *amplitude* gain factor, when the acoustic wave is on exact resonance ($\Delta\omega+\partial\psi/\partial t=0$), thus becomes $e^{(a\Gamma T_2' N_z)\zeta}$. The results are easily generalized for the case of an inhomogeneous line made up of a number of spin packets. For a distribution of spin packets which is symmetrical about the frequency $\omega-\partial\psi/\partial t$ of the incident wave there is no resultant phase shift and the amplitude gain constant can be written as

$$a\Gamma T_2'\int\frac{N_{z,\omega'}d\omega'}{1+(T_2'\omega')^2} \quad ,$$

where

$$\omega'=\Delta\omega+\frac{\partial\psi}{\partial t}$$

and $N_{z,\omega}$ denotes the excess spin population per cm^3 per unit spectral interval (in rad/sec units). If the linewidth $\gg 1/T_2'$, $N_{z,\omega}$ can be taken outside the integral and we derive an amplitude gain constant with respect to distance traveled:

$$a_\zeta=\pi a\Gamma N_{z,\omega}=\frac{\pi(G\mu_B H_0)^2\omega N_{z,\omega}}{4\sqrt{2}\,\rho v^3\hbar} \quad . \tag{3.14}$$

The corresponding amplitude gain constant with respect to time is $\alpha_t=v\alpha_\zeta$. Power gain constants are $2\alpha_\zeta$ and $2\alpha_t$.

The gain is a function of the position in the resonance line and also of the degree of burn out as described by the parameter $N_{z,\omega}$. Since $N_{z,\omega}$ changes with time the amplification of a wave is therefore not linear in the strict mathematical sense. We can, however, assume the principle of superposition in our treatment without introducing serious errors so long as the condition (3.10) holds good. Then, by Eq. (3.11), $N_{x,\omega}$ and $N_{y,\omega}$, which determine the rate of growth of the wave, are proportional to the value of $N_{z,\omega}$ at any moment and we can make a Fourier decomposition of the wave into frequency components and compute the amplified signals independently of one another. Since the approximation which we have made in Eq. (3.11) is equivalent to using a "transition-probability" model[30] we can conveniently describe this as the transition-probability approximation. The situation is entirely different if $\Gamma s T_2'\gg 1$. Growth of the wave and the magnitudes of N_x, N_y

(which may now exceed N_z) become dependent on the way in which the two-level system was prepared at an earlier time. There will be considerable cross coupling between frequency components and Fourier decomposition of the wave and calculation of the individual responses no longer affords a valid procedure.

We pause here and estimate some orders of magnitude for samples of the kind which we have used in our experiments. In order to have some definite point of reference we assume the following experimental conditions: $\omega_0/2\pi = 9.1$ GHz, $T = 1.4$ °K, $N = 10^{19}$ spins/cm^3, resonance line Lorentzian in shape with a half-width at half-height $\Delta\omega_L/2\pi = 12\frac{1}{2}$ MHz (corresponding to a full width at half-height ~10 G). Under these conditions the excess number of spins/cm^3 in the lower state in Boltzmann equilibrium $N\tanh(\hbar\omega/kT) = 1.58\times10^{18}$; the excess spin concentration per unit spectral interval at the line center $N_{z,\omega,0} = N\hbar\omega/2kT/\pi\Delta\omega_L = 6.4\times10^9$ sec. For the remaining material parameters we adopt the values[31-33] $v = 2\times10^5$ cm sec^{-1}, $\rho = 2.1$, and $1/TT_{1d} = 41$ deg^{-1} sec^{-1} at 9.1 GHz. From Eq. (3.5) we thus obtain $G\mu_B H_0 = 6.53\times10^{-16}$ erg, which, by Eq. (3.6), leads to a nutation constant $\Gamma = 6.2\times10^{11}$ sec^{-1} [$\Gamma/2\pi = 99$ kHz per microstrain (10^{-6} strain) unit]. According to Eq. (3.14) the power gain constants for a 100% efficient inversion are $2\alpha_\xi = 10$ cm^{-1} or $2\alpha_t = 2.0$ μsec^{-1}. In practice we have been able to obtain inversion efficiencies ~80% corresponding to power gain constants of ~8 cm^{-1} or 1.6 μsec^{-1}.

It is useful to have an ideal of the over-all gain G_p which takes place before the thermal noise field initially present in the sample reaches high enough intensity to cause observable burn out of the electron-paramagnetic-resonance (EPR) line. It is also of some importance to know approximately what strain amplitudes s are generated in the process so that we can see, from Eq. (3.10), whether the transition-probability analysis is likely to be valid. As shown in the theory of specific heats the energy/cm^3 per unit spectral interval in thermal equilibrium due to the two transverse modes is given by $E_{\omega,0} = \hbar\omega^3/[\pi^2v^3(e^{\hbar\omega/kT}-1)]$. The acoustic energy $E_{\omega,1/2}\delta\omega$ present at the midavalanche point can be found by equating $E_{\omega,1/2} - E_{\omega 0}$ with the energy per unit spectral interval $\frac{1}{4}\hbar\omega_0 N_{z,\omega,0}$ discharged by the spin system and inserting the appropriate avalanche bandwidth $\delta\omega$. [The fraction of energy lost $\simeq (T_{\text{phonon}}\times 2\alpha_t)^{-1} \approx 2\%$ and can be ignored.] We thus find that the ratio between the acoustic energy in midavalanche and the acoustic energy initially present

$$E_{\omega,1/2}/E_{\omega,0} = G_p = 1 + \pi^2 N_{z,\omega,0} v^3 (e^{\hbar\omega/kT}-1)/4\omega^2 = 3\times10^4.$$

This corresponds to ~10 e folds. According to our estimate $2\alpha_t = 1.6$ μsec^{-1} for the power gain factor, it should therefore take ~6 μsec after the 180° spin inversion to reach the midpoint of the avalanche [see Eq. (2.3)]. The observed times were actually about half as long again as this for samples having concentrations and linewidths close to the values assumed here, suggesting that $2\alpha_t \sim 1.1$ μsec^{-1} would be a more realistic value for the power gain constant.

The strain amplitudes reached in midavalanche can be estimated by expressing $E_{\omega,1/2}\delta\omega$ in terms of acoustic strain. Let us suppose that the acoustic field is made up of linearly polarized waves $s_T = 2s\cos(\omega t - \psi - \omega\zeta_i/v)$ of both traverse types traveling in three orthogonal directions ζ_i. Then the acoustic energy/cm^3 is $6\rho v^2 s^2$. Equating this to $\frac{1}{4}\hbar\omega_0 N_{z,\omega,0}\delta\omega$ (i.e., to the spin energy release) we have $s^2 = (3\hbar\omega_0 N_{z,\omega,0}\delta\omega)/2\rho v^2$. Inserting numerical values ($\delta\omega/2\pi \simeq 10$ MHz) we obtain $s \sim 3.4\times10^{-6}$. The corresponding nutation frequency $\Gamma s/2\pi$ is 0.34 MHz. If we now take T_2' as the spin-echo phase memory time $T_2 \sim 4$ μsec we obtain $\Gamma s T_2' \sim 9$, which suggests that the transition-probability approximation ceases to be valid sometime before the midavalanche point is reached and that a full nonlinear analysis should be made. However, as we pointed out earlier, T_2' represents the relative coherence time of the spin system and of the fluctuating acoustic field responsible for driving it. This value of T_2' will be shorter than the value of T_2 which measures the coherence of the spin system in relation to a monochromatic rf field.

Because of the large over-all gain which takes place, even before there is any appreciable burn out of the line, it is fairly easy to predict the form of the acoustic spectrum which is generated at this stage, irrespective of the line shape. The initial acoustic spectrum $E_{\omega,0}$ is essentially flat over the region concerned. The spectrum E_ω developed during the avalanche will therefore have the same form as the power gain factor $e^{2\alpha_t t} = e^{2\pi a\Gamma N_{z,\omega} vt}$. This expression is a strong function of $N_{z,\omega}$ and depends primarily on the line shape near the peak of the line which can be approximated by a parabola. For a Lorentzian line we have $N_{z,\omega,0} \simeq N_{\max}\times[1-(\Delta\omega/\Delta\omega_L)^2]$. The acoustic spectrum for times which occur several exponential gain periods after the start of the avalanche (but which do not extend into the range where significant burn out occurs) is therefore given by

$$\exp(2\pi a\Gamma N_{z,\omega,0} vt)$$
$$= \exp(2\pi a\Gamma N_{\max} vt)\exp\{-[(\Delta\omega/\Delta\omega_L)^2 2\pi a\Gamma N_{\max} vt]\}\ . \quad (3.15)$$

At the peak of the acoustic spectrum $E_\omega = E_{\max} = E_{\omega,0}\exp(2\pi a\Gamma N_{\max} vt)$. The form of E_ω given by $E_{\max}\exp[-(\Delta\omega/\Delta\omega_G)^2]$, where

$$\Delta\omega_G = \Delta\omega_L/(2\pi a \Gamma N_{\max} v t)^{1/2} , \quad (3.16)$$

i.e., the ratio between the width of the initial inverted line and the width of the acoustic spectrum is approximately given by the root of the power gain exponent. For our set of numerical values the ratio $\Delta\omega_L/\Delta\omega_G \sim 2.5$ to 3 when the acoustic intensity corresponding to visible burn out is reached. The result is fairly insensitive to errors made in estimating the over-all power gain. It must, however, be modified by inserting a reduced value of $\Delta\omega_L$ if the 180° pulse inverts less than the full line (see Fig. 7).

The result (3.16) enables us to form an estimate of the coherence time which characterizes the spin-phonon interaction. The Fourier transform of the power spectrum $\exp[-(\Delta\omega/\Delta\omega_G)^2]$ yields the autocorrelation function $\exp[-(\Delta\alpha_G^2 t^2/4)]$. The autocorrelation time $t_c \simeq 2/\Delta\omega_G \simeq 6/\Delta\omega_L$ is a measure of the time which the phase ψ (and the amplitude s) of the strain energy undergoes a random change in any small volume of the sample. These random fluctuations must be taken into account in calculating the decay constant T_2' used in (3.7) and in the test expression (3.10). Ideally a convolution of the phase memory decay function and the acoustic autocorrelation function should be made in order to derive the appropriate decay time. However, since t_c ($\sim 6/\omega_L \sim 76$ nsec) is short[34] compared with T_2 (~ 4 μsec), and since we are only concerned with the approximate order of magnitude in applying the test (3.10), it will suffice to write $1/T_2' = 1/T_2 + 1/t_c$. Using the previously estimated magnitude $s = 3.4\times10^{-6}$ for the strain amplitude in midavalanche we thus obtain $\Gamma s T_2' \sim 0.16$. Even allowing for some margin of error in the estimates of Γ, s, T_2' and for some changes in s and T_2' as the avalanche develops, it seems that we shall therefore be reasonably well justified in using the transition-probability approximation to treat our standard case. However, since a change in the conditions of the experiment could easily modify both T_2' and s, we shall briefly review the question of nonlinear interactions between the acoustic field and the two-level system later on (Sec. III C).

We now calculate the form of the hole which is burnt out in the resonance line. According to the transition-probability approximation the acoustic energy E_ω per unit spectral interval grows according to the equation

$$\frac{dE_\omega}{dt} = E_\omega \times 2\pi a \Gamma N_{z,\omega} v = 2\alpha_{t,\omega} E_\omega \frac{N_{z,\omega}}{N_{z,\omega,0}} , \quad (3.17)$$

where $2\alpha_{t,\omega}$ is the power gain constant before burn out [see Eq. (3.14) *et seq.*]. The phonon lifetime experiments show that the sum of the spin and phonon energies remains approximately constant. Thus

$$E_\omega + \tfrac{1}{2}\hbar\omega N_{z,\omega} = W_\omega , \quad (3.18)$$

where W_ω is the total available avalanche energy at a frequency $\omega+\Delta\omega$ in the resonance line. Solving (3.17) and (3.18) we obtain

$$E_\omega/W_\omega = \tfrac{1}{2}\{1+\tanh[\alpha_{t,\omega}(t-t_{1/2,\omega})W_\omega/\tfrac{1}{2}\hbar\omega N_{z,\omega,0}]\} ,$$

$$N_z\hbar\omega/2W_\omega = \tfrac{1}{2}\{1-\tanh[\alpha_{t,\omega}(t-t_{1/2,\omega})W_\omega/\tfrac{1}{2}\hbar\omega N_{z,\omega,0}]\} ,$$

where $t_{1/2,\omega}$ is the avalanche half-fall time at which the available energy is equally divided between the spins and the acoustic field. As we have seen earlier the initial acoustic energy $E_{\omega,0}$ is $\sim 10^{-4}$ of the total available energy. We can therefore approximate $\frac{1}{2}\hbar\omega N_{z,\omega,0} \simeq W_\omega$ and rewrite the above equations in the form

$$E_\omega = \tfrac{1}{2} W_\omega[1+\tanh\alpha_{t,\omega}(t-t_{1/2,\omega})] , \quad (3.19)$$

$$N_{z,\omega} = \tfrac{1}{2} N_{z,\omega,0}[1-\tanh\alpha_{t,\omega}(t-t_{1/2,\omega})] . \quad (3.20)$$

The half-fall time at any point in the spectrum can be inferred from the initial acoustic power spectrum present at the time t_0 of the inverting pulse. From (3.19) we have

$$\begin{aligned}\alpha_{t,\omega}(t_{1/2,\omega}-t_0) &= \tanh^{-1}(1-2E_{\omega,0}/W_\omega)\\ &= \tfrac{1}{2}\ln(W_\omega/E_{\omega,0}-1)\\ &\simeq \tfrac{1}{2}\ln(W_\omega/E_{\omega,0}) . \end{aligned} \quad (3.21)$$

Combining this with Eqs. (3.19) and (3.20) we have

$$E_\omega = \tfrac{1}{2} W_\omega\{1+\tanh[\alpha_{t,\omega}(t-t_0) - \tfrac{1}{2}\ln(W_\omega/E_{\omega,0})]\} , \quad (3.22)$$

$$N_{z,z} = \tfrac{1}{2} N_{z,\omega,0}\{1-\tanh[\alpha_{t,\omega}(t-t_0) - \tfrac{1}{2}\ln(W_\omega/E_{\omega,0})]\} . \quad (3.23)$$

The half-fall time $T_{1/2} = t_{1/2} - t_0$ described in the experimental section is given by

$$\begin{aligned}T_{1/2} &= (1/2\alpha_{t,\text{peak}})\ln(W_{\text{peak}}/E_0)\\ &\simeq (1/2\alpha_{t,\text{peak}})\ln(S_{\text{peak}}) , \end{aligned} \quad (3.24)$$

where S_{peak} is the ratio of the available spin energy to the initial phonon energy (per unit spectral interval), and where α_t, W_ω have been assigned values which correspond to the center of the resonance line. ($E_{\omega,0} = E_0$ represents the initial white noise spectrum which is flat.) The spectral form of E_ω and $N_{z,\omega}$ in Eqs. (3.22) and (3.23) can be calculated by substituting appropriate distribution functions for $\alpha_{t,\omega}$, W_ω, $N_{z,\omega,0}$. For instance, if the resonance line is Lorentzian $\alpha_{t,\omega} = \alpha_{t,\text{peak}} L_\omega$, $W_\omega = W_{\text{peak}} L_\omega$, $N_{z,\omega,0} = N_{z,\text{peak},0} L_\omega$, where $L_\omega = \Delta\omega_L^2/(\Delta\omega_L^2 + \Delta\omega^2)$ and $\alpha_{t,\text{peak}}$, W_{peak}, $N_{z,\text{peak}}$ are values corresponding to the center of the line. In some circumstances a parabolic approximation may be more convenient. The results calculated by (3.22) and (3.23) are, of course, only approxi-

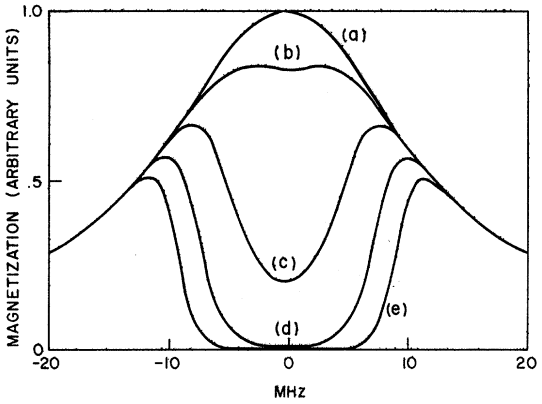

FIG. 10. Burn out of resonance line according to transition-probability theory [Eq. (3.23)]. Full width at half-height of resonance line is 25 MHz. Power gain constant $2\alpha_t = 2\ \mu\text{sec}^{-1}$ at center of line. (a) Acoustic energy/spin energy ~ 0.01 in center of line; burn out negligible, (b)–(e) burn out 1.5, 3.0, 4.5, 6.0 μsec later. (Initial ratio of acoustic energy/spin energy $\sim 0.3\times 10^{-4}$.)

mate in any case since they assume an infinite phonon lifetime. Experiments suggest that this assumption does not introduce serious errors during the first half of the avalanche, but that it is a poor one to make for the latter half. This point is taken up again in Sec. IV.

Some examples of burn-out spectra calculated from (3.23) for the case of a Lorentz line are shown in Fig. 10. Figure 11 gives the corresponding Fourier transforms. Comparison may be made between these Fourier transforms and the experimental free-induction signals in Fig. 6. The acoustic energy spectrum [Eq. (3.22)] is merely

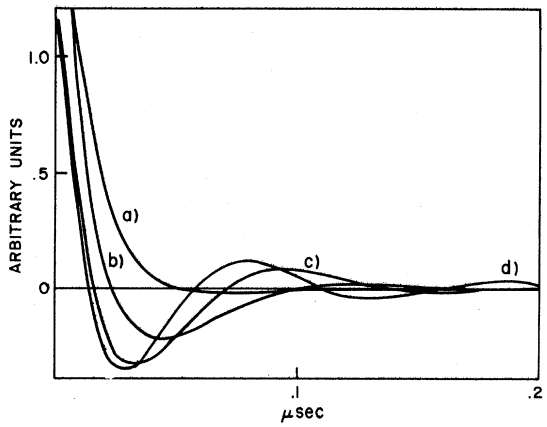

FIG. 11. Fourier transforms of burnt-out lines (b)–(e) in Fig. 10. (a) is FT of (b), etc. These curves correspond to the free-induction signals which would be generated by an ideal 90° pulse. (Compare with experimental curves in Fig. 6.)

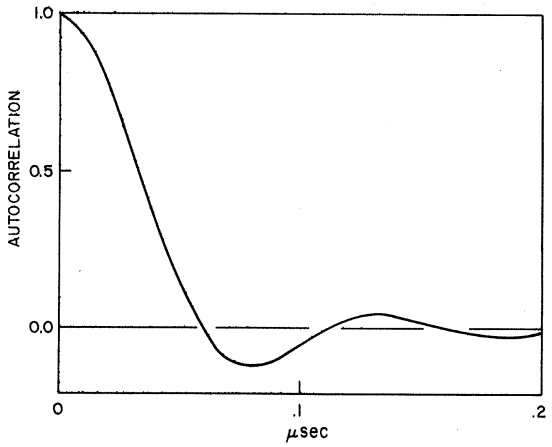

FIG. 12. Autocorrelation function of acoustic field generated during avalanche burn out shown in Fig. 10(e).

proportional to the holes burnt in the Lorentzian line and is not shown. Its Fourier transform gives the acoustic autocorrelation function as shown in the example in[35] Fig. 12.

The presence of an acoustic power spectrum with an autocorrelation function such as that shown in Fig. 12 can be used to explain the result obtained in the modified burn-out experiment reported in Sec. II C. If the Zeeman field is suddenly changed so that an unburnt spectrum of spin packets $N'_{z,\omega,0}$ is moved into resonance with the acoustic field E_ω, a burn-out pattern which to the first order is proportional to E_ω will appear. A 90° microwave pulse applied to the resulting spin spectrum will generate a free-induction signal which is proportional to the difference between the Fourier transform of $N'_{z,\omega,0}$ and the Fourier transform of E_ω, i.e., to the Fourier transform of the unburnt spin spectrum superimposed on the acoustic autocorrelation function. If the spectral width of $N'_{z,\omega,0}$ is large compared with the spectral width of $E_{\omega,t}$ the tail of the free-induction signal will once again be dominated by a periodicity as in Figs. 11 and 12.

C. Nonlinear Interaction between Spins and Acoustic Waves

In Sec. III B we estimated that the product $\Gamma s T_2'$ reached a value $\lesssim 0.2$ in midavalanche and concluded that the transition-probability approximation would remain valid throughout the avalanche. This assumption now seems to be confirmed by the similarity between the experimental free-induction signals and the calculated curves in Fig. 11. We must point out, however, that the form of the free-induction signal is not quite as decisive a confirmation as it might appear, and that the case for a transition-probability interpretation rests primarily on our estimates of Γ, s, T_2'. Free-induction traces of a very similar form would probably ap-

pear even if the interaction were fully nonlinear.

Analytic solutions generally cannot be obtained in the nonlinear regime, and, to explore the situation, we have had to resort to numerical computations. In these computations, the physical situation was simulated by allowing various waveforms $s(t)$ to be incident on a boundary $\zeta = 0$ in a medium containing a uniformly inverted spin population. The spectral distribution of spin packets was taken to correspond to the portion of an inhomogeneous Lorentz line lying between two half-amplitude points. The evolution of $s(t)$ was then followed for successive elements $\Delta\zeta$, i.e., as a function of the distance traveled in the medium.[36]

We have taken a variety of different shapes for the incident waveform $s(t)$ (including some sample noise waveforms). In all cases the results had certain features in common. As long as the chosen waveform $s(t)$ remained at a level such that $\int \Gamma s\, dt \ll 1$ the computation merely yielded amplified waveforms of the same general shape. Sharp edges were, however, rounded and noise waveforms were partially smoothed as one would expect from the narrowing of the bandwidth discussed earlier [Eq. (3.16)]. At higher power levels as $\int \Gamma s\, dt$ approaches π the waveform acquired an oscillatory tail.[37] Further evolution tended to conserve this area and reproduced waves with the same oscillatory feature.[38]

As an illustration let us consider the amplification of the Gaussian wave shown in Fig. 13(a). The parameters a, Γ, v were chosen to be the same as in our previous estimate. We have, however, assumed that the inverted portion of the line was only $\sim\frac{1}{10}$ of the full line (as, for example, in some of the tests discussed in Sec. II C) and chosen the acoustic autocorrelation time of our sample waveform accordingly. (A longer acoustic autocorrelation time brings about a situation in which the limit of the validity of the transition-probability model is approached without the need for wholesale alterations in all the other parameters.) The autocorrelation time of the input Gaussian wave is 1.4 μsec. Since the choice of waveform automatically sets the appropriate limit on the coherence time t_c was not used for T_2' in this simulation. Instead we set $T_2' = T_2 = 3$ μsec. [Since T_2' is longer than the autocorrelation time of the sample input wave $s(t)$ it actually has comparatively little effect on the evolution of the waveform.] Nonlinearly amplified waves are shown in Figs. 13(b)–13(d) and illustrate the course of events which we described above. The area under the final curve in Fig. 13(d) is $\simeq 0.9\pi$. The peak strain of 10^{-5} is higher than the value 3.4×10^{-6} which we estimated earlier and is indicative of how much more spin energy (or what margin of error in the earlier estimate[39]) would be needed to render the spin-phonon interaction fully nonlinear.

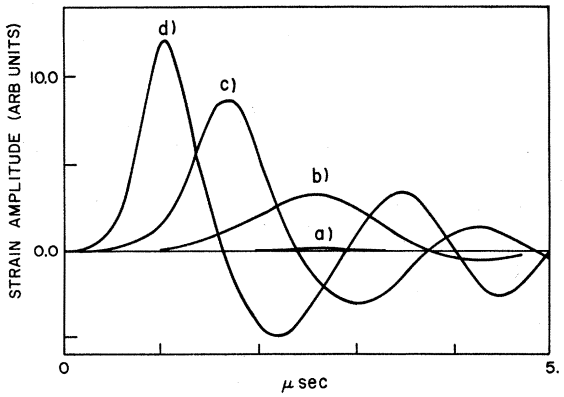

FIG. 13. Amplification, according to the full nonlinear theory, of a traveling wave initially characterized by a Gaussian envelope. Parameters $\Gamma = 6.2\times10^{11}$, $a = 5.5\times10^{-22}$, $N_{z,\omega,0} = 6.4\times10^{9}$ as estimated in text for a typical LMN+Ce sample. $T_2' = 3$ μsec.

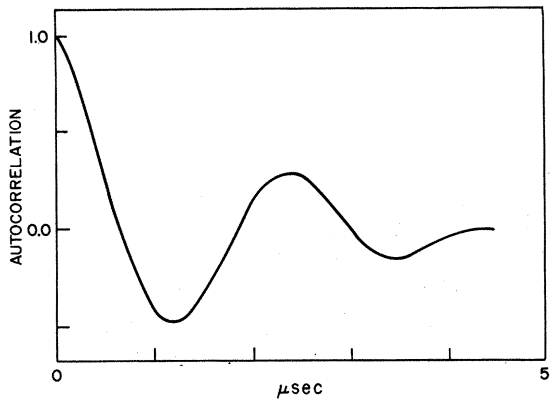

FIG. 14. Autocorrelation function for wave in Fig. 13(d). Compare with Fig. 12 (i.e., autocorrelation for acoustic spectrum calculated according to transition-probability theory).

If the acoustic field consisted of a number of π pulses, all closely resembling one another, it is easy to argue that the free-induction signal generated by the hole burnt in the line would have the familiar periodic tail. The argument can be applied in its most simple form to the "modified" experiment described in Sec. II C. The π pulses would burn out a hole (in the side of the line) proportional to the Fourier transform (FT) of this power spectrum, i.e., to the autocorrelation function of acoustic pulses themselves. The autocorrelation function for the final curve in Fig. 13(d) is shown in Fig. 14. It is similar to the autocorrelation obtained (Fig. 12) by means of the transition-probability analysis and is qualitatively in agreement with the observed induction signals.

Some doubt may arise as to whether an average over many such autocorrelation functions, arising from the superposition of π pulses of slightly differing shapes, would still give rise to the periodicity in the tail. This cannot easily be settled by further computation, but one can at least produce a plausible reason why this should be so as follows. The first π pulses originate from large-amplitude fluctuations in the acoustic noise waveform.[40] Once formed they grow only linearly with distance traveled (taking all the spin energy in their path), whereas the rest of the noise waveform continues to grow exponentially. The π pulses which are formed initially therefore change relatively slowly while large numbers of new π pulses join the population, the result being an accumulation of pulses with a particular range of intensities and with broadly similar waveforms.

The computations are open to yet another objection which can only be met by means of qualitative arguments. It has been assumed that a pulse encounters an "unused" inverted resonance line as it traverses the medium. This may be roughly justified by picturing the medium as a volume containing a relatively low density of large-amplitude pulses analogous to the atoms of a perfect gas. Unfortunately the density cannot remain low as the avalanche evolves and it is difficult to envisage what will happen as pulses begin to cross one another's tracks. Our attempts to find a reasonably economic method of simulating the actual situation, taking account of partial burn out of the medium and yet distributing the burn out in a spatially random manner, have not met with great success. This and other variations on the problem would in any case lead to an expenditure of time and money which hardly seem to be justified in view of the apparently secondary importance of nonlinear effects in our particular material. Should nonlinear interactions prove to be important in other materials the extensive and growing volume of calculations in the laser field should be useful in providing the necessary insights.

IV. DISCUSSION

A. General

In the early stages of this experimental program it seemed that it would only be possible to explain the situation in midavalanche in terms of the nonlinear spin-phonon interaction. The periodicities observed in the tail of the free-induction signal strongly resembled the periodicities obtained in nonlinear computations of the acoustic waveform, and the measured value of the spin-echo phase memory time T_2 seemed to ensure [Eq. (3.10)] that the linear limit would be exceeded before burn out became appreciable. We have, however, argued in Sec. II B that T_2 does not give the correct value of T_2' to be used when an amplified noise field rather than a monochromatic signal is responsible for spin nutation, and that a time approximately equal to the autocorrelation time of the field should be used in (3.10) instead. Also we have shown that the periodicities can be adequately explained without recourse to a full scale nonlinear theory. The choice of an interpretation remains somewhat arbitrary, especially in the case where only a small fraction of the line is inverted thus giving rise to longer acoustic autocorrelation times, and, as we have pointed out, it rests largely on the approximate estimates for the spin lattice coupling parameter G and for the strain amplitude s. But the transition-probability approximation has the great merit of producing a solution in closed form which is adequate to explain the data. It is not at all certain that nonlinear theory, based on the computation of special cases, could provide as satisfactory an explanation.

The equations derived in Sec. II B can easily be shown to be equivalent to the equations given by Brya and Wagner. If we take Eqs. (1a) and (1b) of Ref. 1 and let the spin lattice time due to other than direct processes T_{1I} and the phonon lifetime T_p tend to infinity we can integrate these equations to give

$$u = \tfrac{1}{2}\{1 - \tanh[(S/2T_1)(t - t_{1/2})]\} \quad , \tag{4.1}$$

where S is the ratio between the spin energy and the energy in the resonant lattice modes in thermal equilibrium. u is the same as $N_z/N_{z,0}$ in our analysis, $t_{1/2}$ is a constant of integration, and Eq. (4.1) is the same as Eq. (3.20) with the power gain constant $2\alpha_t$ replaced by S/T_1. The value of S/T_1 (T_1 recomputed at 9.1 GHz) in Ref. 1 is $\sim 1.4\ \mu\text{sec}^{-1}$ and is not materially different from the value $2\alpha_t \sim 2.2\ \mu\text{sec}^{-1}$ which we derive here. A significant difference does, however, appear in the phonon lifetime which we measure to be $\sim 20\ \mu$sec and which was taken as $\sim 1\ \mu$sec in[41] Ref. 1.

It is perhaps surprising that the long phonon lifetime was not manifested as a severe "phonon bottleneck" in the relaxation experiments reported by Brya and Wagner. The bottleneck is usually characterized by a parameter σ, where σ is the ratio of phonon energy gain from the spin system to phonon energy loss (Ref. 1, p. 402). It leads to a lengthening of the observed recovery time in a spin lattice relaxation experiment such that $T_1(\text{observed}) = (\sigma + 1)T_1$. If we take a gain parameter of 1.6 per μsec and a phonon lifetime of 20 μsec we obtain the value $\sigma = 32$. On the other hand Brya and Wagner's relaxation measurements[42] on the same system show a much weaker bottleneck with σ typically 2 or 3.

Brya and Wagner suggest that their interpretation

of the data could be affected by cross relaxation. This suspicion is borne out by some tests we were able to make on our samples indicating that the resonance line, if initially excited in a nonuniform manner, was homogenized (over a spectral interval ~100 MHz) in times $\sim T_1$. In this case the value of σ appropriate to the avalanche will be that at the center of the line, where the spectral density and hence the gain is highest, whereas the relevant value of σ in the recovery to equilibrium will be an average over some effective homogeneous width. A meaningful estimate of the reduced bottleneck would require a much better understanding of cross relaxation than presently exists. However, a consideration of the magnitudes involved indicates that no serious conflict exists.

B. Role of Phonon Lifetime and of Cross Relaxation in Modifying the Form of Avalanche Curve

Our procedure in setting $T_{ph} \to \infty$ affords a good approximation in the initial portion of the avalanche but a bad one in the tail. From Eq. (3.20) when $t \ll t_{1/2}$, we have

$$N_{z,\omega}/N_{z,\omega,0} \simeq 1 - \exp[2\alpha_t(t - t_{1/2})] \ . \tag{4.2}$$

Hence (assuming conservation of the total energy), the phonon intensity is growing according to the factor $e^{2\alpha_t t}$, i.e., the fractional rate of increase is $2\alpha_t$. In order to correct for phonon loss we should reduce $2\alpha_t$ to $2\alpha_t - 1/T_{ph}$. The fractional correction $1/2\alpha_t T_{ph}$ is ~2% and is negligible in comparison with other uncertainties.

The effects of phonon loss may show up more readily in the tail of the avalanche. In the absence of any loss the avalanche will be described by $N_{z,\omega}/N_{z,\omega,0} \simeq e^{[-2\alpha_t(t-t_{1/2})]}$ [as we can see by setting $t - t_{1/2} \gg 1$ in Eq. (3.19)], and the fractional rate of change will be given by

$$\frac{1}{N_{z,\omega}} \frac{dN_{z,\omega}}{dt} = -2\alpha_t \ . \tag{4.3}$$

The decay of $N_{z,\omega}$ arises as a result of the progressive saturation of the spin system by a phonon field which, according to our assumption of energy conservation, is of approximately constant intensity and contains all the energy initially present in the spin system. If we now suppose instead that there has been a loss of energy, which at time t can be denoted by the loss factor $q_\omega(t)$, then (4.3) becomes

$$\frac{1}{N_{z,\omega}} \frac{dN_{z,\omega}}{dt} = -\frac{2\alpha_t}{q_\omega(t)} \ . \tag{4.4}$$

We should therefore be able to determine the phonon loss by comparing the decay constant $(1/N_{z,\omega}) \times (dN_{z,\omega}/dt)$ at various points in the tail of the avalanche with the gain constant observed at the beginning. In particular by writing

$$q_\omega(t) = q_\omega(t')e^{(t-t')/T_{ph}} \ , \tag{4.5}$$

we should be able to separate out the loss $q_\omega(t')$ occurring during the main portion of the avalanche (ending as t') from the loss occurring when little or no extra energy is being contributed by the spin system. The latter factor should, as indicated in Eq. (4.5), result merely from the exponential decay of the phonon field.

In Fig. 15 we show a sample avalanche curve[43] fitted to the expression $(M_{z,\omega}/M_{z,\omega,0}) = \frac{1}{2}\{1 - \tanh[\alpha_t \times (t - t_{1/2})]\}$. $t_{1/2}$ occurs 8 μsec after the inverting pulse and the power gain constant[44] $2\alpha_t = -0.8$ μsec^{-1}. The fit to the first portion of the curve is good, but the actual values of $T_{1/2}$ and $2\alpha_t$ are hard to explain in terms of the initial ratio S of spin to acoustic energy. Using these values in Eq. (3.24) we should obtain $S = e^{2\alpha_t T_{1/2}} = e^{6.4} = 602$, whereas as we have indicated in Sec. II B a ratio $> 10^4$ is more in line with expectations. A more striking discrepancy occurs in second half of the avalanche. Suppose now we try to explain this solely in terms of phonon decay. The apparent loss factor $q(t')$, derived by comparing the acoustic gain constant at ~4 μsec after the avalanche with the magnetization decay constant ~11 μsec after the avalanche, is ~4:1, and the phonon decay time inferred from the tail itself[45] is ~9 μsec. This latter value is ~ half the value measured (for the same sample) by the method of Sec. II B. Moreover, even if we assume that the true phonon decay time is 9 μsec, and not 20 μsec as obtained by the Sec. II B experiment, we still are unable to account for the value of $q(t')$ by phonon decay.

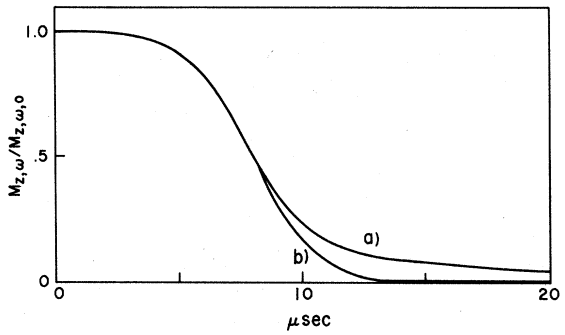

FIG. 15. (a) Experimental avalanche curve for 0.5% sample. (b) Ideal curve $1 - \tanh[\alpha_t(t - t_{1/2})]$ where $t_{1/2} = 8$ μsec and $2\alpha_t = 0.8$ μsec. Although these parameters give a good fit in the first half of the avalanche there is reason to suppose that $2\alpha_t$ is not the true power gain constant and that 8 μsec is not the ideal half-full time according to transition-probability theory. The discrepancy is probably due to spectral diffusion. The difference between curves (a) and (b) for the latter half of the avalanche is due partly to spectral diffusion and partly to phonon decay.

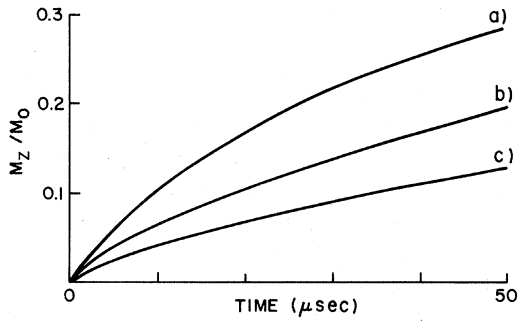

FIG. 16. Graph showing filling in of holes burnt in the resonance line of a 0.5% LMN Ce sample by a 90° pulse. (a) $\omega_1/2\pi = 2.5$ MHz (hole ~7 MHz full width at half-depth), (b) $\omega_1/2\pi = 5$ MHz, (c) $\omega_1/2\pi = 10$ MHz.

The measurements made on the tail, and the implausibly small value of S esimated from $2\alpha_t T_{1/2}$, both suggest that phonon decay cannot be the only factor modifying the avalanche curve from the idealized tanh shape. We turn therefore once again to cross relaxation. This process was clearly responsible for distorting the avalanche curves obtained in the more concentrated samples right from the outset. The distortion of the curves in the dilute samples was much less obvious, but it may well have led to a fit (to the first half of the curve) being made with too small a value of α_t. Retaining $T_{1/2} = 8$ μsec but setting $S = 2.2 \times 10^4$ we should infer a gain constant $2\alpha_t = 1.25$ μsec^{-1}, or ~1.5 × the value used in the fit. More realistically yet, reducing $T_{1/2}$ to ~6 μsec to bring the idealized curve entirely below the experimental curve, we should infer a gain constant ~1.7 μsec^{-1}.

As stated earlier we have not been able to give a quantitative explanation of these cross-relaxation effects and we limit ourselves to presenting a measurement to indicate that they are at least of the right general order of magnitude. Figure 16 shows the rate of filling in of holes burnt in the resonance line of the 0.5% sample for which the avalanche curve has just been discussed. The holes were burnt by applying 90° pulses with suitably chosen values of H_1 and the fill-in was observed as a function of time by monitoring with a two-pulse sequence. The width of a typical avalanche hole lies somewhere between the holes generated by $\omega_1/2\pi = 5$ MHz and $\omega_1/2\pi = 2.5$ MHz. The initial filling-in rate $(1/M_z)(dM_z/dt)$ for a hole of this width is ~1% per μsec.

It does not appear that this rate is sufficiently rapid to explain the discrepancy between curves (a) and (b) in Fig. 15. Even less, it is able to explain the difference between the experimental curve (b) and any theoretical curve which might be drawn with the value of $2\alpha_t$ and $T_{1/2}$ realistically revised as suggested above, We do not know the reason for this. It seems possible, however, that the spectral diffusion process is accelerated during the avalanche and causes filling in to take place somewhat more rapidly under these conditions than it does under test conditions. Spectral diffusion originates in the local field changes which occur when the spins in an environment change their orientation. These changes of orientation are primarily due to spin-spin flips in LMN + Ce at 1.4 °K, but they will be accelerated if the spin system is driven by an external field. Some evidence for accelerated spectral diffusion due to rf fields exists (viz., the instant diffusion process mentioned in Sec. II D) and we are merely suggesting here that in the avalanche, acoustic fields may play a similar role.

C. Possible Effects of Anisotropy

In our treatment of the interaction of the acoustic waves with the spin system we represented the spin lattice coupling by a single parameter G and assumed that the LMN crystal was elastically isotropic. This enabled us to discuss the avalanche buildup in a relatively simply manner, and was in any case the best we could do since the individual components of the elastic tensor and of the spin lattice coupling tensor have not been measured. One might ask, however, if a more detailed consideration of the anisotropies in the problem would not change the interpretation of the data in some important way.

To see if this is likely to be so, let us consider a hypothetical situation in which half the lattice modes (modes A) are strongly coupled to the spin system and the other half (modes B) are coupled weakly or not at all. From T_1 we should then derive a coupling constant $G(\text{modes } A) \simeq \sqrt{2}G$ (average over all modes). $\Gamma(\text{modes } A)$ would be $\simeq \sqrt{2}\,\Gamma$ (average), and the gain parameters $\alpha(\text{modes } A) \simeq 2\alpha(\text{average})$. If there were no acoustic coupling between the two types of modes the avalanche would concern modes A only and would take place twice as fast as we have assumed. The nonlinearity test expression $\Gamma_S T_2'$ [Eq. (3.10)] would be $\sqrt{2}$ times as large as in the averaged out case.

In practice, of course, energy is likely to be transferred from modes A to modes B at each boundary reflection in the LMN crystal. In our sample these reflections occur on the average ~2 mm from the point where the acoustic energy is emitted thus suggesting that the mode transfer time t_{AB} will be several μsec. However, even if transfer were highly probable at each reflection so that $t_{AB} \simeq 1$ μsec, the avalanche would build up in much the same way as if modes B were entirely decoupled. This is because the growth of energy in modes B is delayed, causing the energy density

in modes B (during the early part of the avalanche) to be less by a factor $\sim \exp[2\alpha_t(\text{modes } A)t_{AB}] \sim 25$. In the later stages of the avalanche, where little acoustic gain is taking place, the energy would tend to be equalized, leading to a net loss of energy from modes A and an appropriately reduced burn-out rate for the spins.

The above example illustrates the following three ways in which the theoretical predictions might be modified if there were strongly preferential coupling into a fraction of the total lattice modes: (a) The first portion of the avalanche would take place at a rate more rapid than the rate we have estimated in Sec. III B; (b) there would be more likelihood of the interaction becoming nonlinear; and (c) there would be an apparent loss of acoustic energy between the initial and final portions of the avalanche. Our measurements of $T_{1/2}$ tend to contradict (a). Prediction (b) probably has little to do with the interpretation of results. Earlier estimates (Sec. III B) suggest that there is a sufficient margin to ensure that $\Gamma s T_2' < 1$ even if Γ is increased by a factor of 2 or 3 for a given set of modes (besides which nonlinearity might not significantly affect the observations, Sec. III C). Of the three predictions (c) appears to be the only one which is positively supported by the results – specifically by our observation that the form of the avalanche curve can be explained by assuming that there is a loss $q(t') \sim 4$ of phonon intensity between the initial and final portions of the avalanche. Earlier we ascribed this effect to distortion of the avalanche curve by cross relaxation. We now see that a contribution may arise from phonon transfer as well. However, no corresponding loss was seen in the phonon lifetime experiments where a transfer $\lesssim 20\%$ of acoustic energy into inactive modes, occurring in a time $\simeq 1$ μsec, would have been easy to see. We therefore remain with our previous explanation of the form of the avalanche curve, and conclude in general that little evidence for anisotropy of the phonon field can be derived from the interpretation of the results presented here.

D. Summary

We have shown that the phonon lifetime in samples of LMN showing a phonon avalanche is long, and that it has little or no influence on the form of the avalanche decay curve. Cross-relaxation effects are larger and determine (a) the limit of concentration at which avalanche effects can be seen by means of 180° pulse experiments, (b) the narrowest spectrum of spin packets which will sustain an avalanche when less than the full line is inverted, and (c) the "anomalous" form of the avalanche tail. The phase memory time for spin packets is comparatively long, but is irrelevant to the question of spin-phonon coherence, this being determined primarily by the autocorrelation time of the acoustic field generated in the avalanche. In view of the short coherence time a transition-probability theory is adequate to describe the spin-phonon interaction. This theory predicts a decay curve of the form $1 - \tanh(\alpha t)$ for the magnetization in the center of the line, modifications of this shape being mainly due to cross relaxation as noted above. The transition-probability theory also gives an adequate account of the form of hole burnt out by avalanche and the form of the acoustic spectrum, both of which can be tested experimentally by a 90° pulse free-induction technique.

ACKNOWLEDGMENTS

We should like to thank William J. Brya and Peter E. Wagner for numerous discussions relating to the phonon avalanche problem. In particular we should like to thank Professor Wagner for giving us the 0.3% sample with which our initial measurements were made.

---

*Present address: Department of Physics, Queen's University, Kingston, Ontario, Canada.

[1]William J. Brya and Peter E. Wagner, Phys. Rev. 157, 400 (1967).

[2]In earlier experiments we encountered difficulties arising from the finite decay time of these fields in the microwave cavity. The difficulty was overcome by slotting the adjacent cavity wall as shown in Fig. 1.

[3]The value of the microwave field H_1 can be inferred by noting that for Ce^{3+} in LMN, $g_{\parallel} = 0.03$ and $g_{\perp} = 1.83$. The quantity actually measured here is, of course, ω_1.

[4]The 120°-120° sequence was used merely for reasons of experimental convenience. Its properties are discussed by W. B. Mims, Rev. Sci. Instr. 36, 1472 (1965).

[5]This portion of the line has a spectral width $\sim 2\omega_1$, where ω_1 corresponds to the reduced H_1 used for the monitoring pulses.

[6]This curve is similar to curves given in Ref. 1, Figs. 7 and 8.

[7]During t_H the spin system will, of course, be in contact with a new band of lattice modes and could in principle initiate a new avalanche. If this occurs it is probably a slow process, since the resonance line is now partially burnt out, and the acoustic field at the new frequency has to build up all over again from thermal noise. In our experiments we have been able to verify that the spin population difference scarcely changes during t_p.

[8]This assumption corresponds to the transition-probability model of the avalanche.

[9]$v_{\text{sound}} \sim 2 \times 10^5$ cm/sec.

[10]For a photograph (obtained with a different sample) see Fig. 2(b) in W. B. Mims and D. R. Taylor, Phys. Rev. Letters 22, 1430 (1969), where a preliminary report of this work was given.

[11]We have tried, unsuccessfully, to obtain a quantitative explanation of this limit by studying the spectral diffusion rate in the resonance line. According to our

estimate, spectral diffusion seemed to be insufficient by a factor ~2. We believe, however, that the explanation is essentially correct, and that the discrepancy arises from the difficulty of parametrizing the spectral diffusion rate in LMN+Ce. The Lorentzian diffusion analysis given by W. B. Mims, K. Nassau, and J. D. McGee, Phys. Rev. 123, 2059 (1961) could not be fitted to the results of stimulated echo measurements which we made on LMN+Ce.

[12]The experiment might ideally be performed by switching a second unused resonance line (e.g., another hyperfine component) into the position previously occupied by the first. Unfortunately LMN+Ce provides no second line for use as a phonon monitor and we were forced to use the tail of the one and only resonance line. In order to preserve the tail from the direct effect of the 180° pulse we reduced H_1 (and lengthened the pulse) when performing this experiment.

[13]For a comparison of induction traces observed in the normal and in the modified experiment see Ref. 10, Fig. 2.

[14]See J. R. Klauder and P. W. Anderson, Phys. Rev. 125, 912 (1962), Eq. (4.24).

[15]The problem of estimating T_2 from the echo decay envelope in the LMN+Ce system at X Band may be appreciated by referring to J. A. Cowan and D. E. Kaplan, Phys. Rev. 124, 1098 (1961), Fig. 4.

[16]The exact adjustment was easily made by testing for the inversion of the spin-echo signal with the current pulse applied during a two-pulse echo sequence.

[17]This, of course, points merely to a shortcoming in our technique. It does not prove that a phonon avalanche would be unobtainable if the line were more efficiently inverted, as, for example, by means of a shorter 180° pulse (with larger power H_1) or by an adiabatic fast passage. Our own studies have been limited by the characteristics of our apparatus and by the fact that the spectral diffusion times shorten more rapidly than the avalanche times as the concentration is increased.

[18]The initial thermal noise power will depend on the temperature and not on the sample. The acoustic power reached and the half-full point will be proportional to the spin concentration.

[19]The two-pulse sequence required ~2 μsec to complete. We have generally assumed that the first microwave pulse of the sequence would arrest the progress of the avalanche by destroying the inversion for the spectral region which is being sampled in the center of the line. This assumption may not be a wholly reliable one. Even a weak continuing avalanche would in a strong sample have a considerable effect on the echo amplitude because of instantaneous diffusion (Sec. II D).

[20]The development of small cracks in the crystal could increase the linewidth. Such cracks would not necessarily slow down the avalanche, however, if the crystallites remained acoustically isolated from one another.

[21]Heating of the lattice phonons reduces the gain G_p which is needed to reach the midavalanche point. According to Eq. (2.2) the fractional reduction is given by $\ln(\text{phonon heating})/\ln G_p$. For the phonon heating ratios which concern us here this reduction is ~10%.

[22]L. M. Frantz and J. S. Nodvik, J. Appl. Phys. 34, 2346 (1963); E. O. Schultz-DuBois, Bell System Tech. J. 43, 625 (1964). The "high level linear" approximation (Sec. III B) is assumed in these two papers.

[23]J. P. Wittke and P. J. Warter, J. Appl. Phys. 35, 1668 (1964).

[24]F. T. Arecchi and R. Bonifacio, J. Quantum Electron QE-1, 169 (1965).

[25]C. L. Tang and B. D. Silverman, in *Physics of Quantum Electronics*, edited by P. L. Kelley, B. Lax, and P. E. Tannenwald (McGraw-Hill, New York, 1966).

[26]F. A. Hopf and M. O. Scully, Phys. Rev. 179, 399 (1969).

[27]A. Icsevgi and W. E. Lamb, Phys. Rev. 185, 517 (1969).

[28]We use ζ rather than z to avoid confusing the direction of propagation of the wave with the axis of quantization of the spin system. The axes of quantization and the axes of wave propagation are entirely unrelated in our isotropic model.

[29]The equations describe the evolution of a complex vector $s_c = s_e^{i\psi}$ which denotes the amplitude and phase of the acoustic field. The equation for s_c is

$$\frac{\partial s_c}{\partial \zeta} + \frac{1}{v}\frac{\partial s_c}{\partial t} = ie^{i\psi} a N_+ \ .$$

[30]This is the model used by Brya and Wagner in Ref. 1. It is also the model used to calculate laser gain in Ref. 22. Subsequent laser calculations (Refs. 23–27) take full account of the nonlinearity of the interaction.

[31]Brya and Wagner (Ref. 1); P. L. Scott and C. D. Jeffries [Phys. Rev. 127, 32 (1962)] assume a value $v = 2.5\times10^5$ cm sec^{-1}. F. I. B. Williams, D. C. Krupka, and D. P. Breen [*ibid.* 179, 255 (1969)] suggest $v = 1.84\times10^5$ cm sec^{-1}. This latter value is inferred from specific-heat data reported elsewhere.

[32]2.1 is the density of $Ce_3Mg_2(NO_3)_{12}\cdot 24H_2O$ as determined by the x-ray measurements of A. Zalkin, J. D. Forrester, and D. H. Templeton, J. Chem. Phys. 39, 2881 (1963). We adopt it for LMN without attempting to correct for the change from Ce to La.

[33]W. J. Brya and P. E. Wagner [Phys. Rev. 157, 400 (1967)] obtain $1/T_1 = 6.02\times10^{-39}v^4T$ for the direct process relaxation rate. This corresponds to $1/T_1 = 41T$ sec^{-1} at 9.1 GHz.

[34]If experiments are made in which only a fraction of the line is inverted we must replace $\Delta\omega_L$ by a smaller number. t_c will then be longer and T_M may not be negligible in comparisons with it.

[35]Since $E_\omega + \frac{1}{2}\hbar\omega N_{z,\omega} \simeq \frac{1}{2}\hbar\omega N_{z,\omega,0}$ the acoustic autocorrelation functions might be inferred from the "free-induction traces" calculated in Fig. 11 by subtracting out the Fourier transform of the unburnt line $N_{z,\omega,0}$, i.e., by subtracting the exponential $e^{-(\Delta\omega_L t)}$.

[36]Appropriate computational procedures have been discussed by the authors referred to in Refs. 23–27 and in particular by Icsevgi and Lamb, Ref. 27. Essentially our procedure was as follows: Time was divided into elements Δt such that $v\Delta t = \Delta\zeta$ and shifted by the transformation $t' = t - \zeta/v$ (i.e., the first time element for any space coordinate $\zeta = n\Delta\zeta$ was taken to correspond to the instant at which the wave front first arrived there). Space and time were thus represented by a numerical lattice, a third dimension being introduced to take account of individual spin packets in the line. At a given coordinate $\zeta = n\Delta\zeta$ the effect of $s(t', \zeta)$ on each of the spin packets was computed by making suitable rotations, etc., of the vector N. A summation over spin packets then yielded resultant values of $N_x(t', \zeta)$, etc., which were used in conjunction with Eqs. (3.9) to calculate the increment $\Delta s(t'\zeta)$ in s. Finally, the sum $s + \Delta s$ was

transferred to the space coordinate $(n+1)\Delta\xi$ where, with a new unused spin packet distribution (consisting at $t'=0$ of the component N_z only), the entire operation was repeated.

[37]The appearance of this oscillatory tail has been noted in many analogous laser calculations. Particular attention is drawn to it in the conclusions of Ref. 27. In Refs. 25 and 26 it is pointed out that it is related to the inhomogeneous broadening of the line.

[38]The gain in energy ($\propto \int s^2\,dt$) is brought about by scaling t to shorter intervals and increasing s.

[39]If we had actually made our earlier calculation using the ten times narrower inverted line we should have deduced a value of only $\sim 10^{-6}$ for s. The margin of error would then have to be $\sim 10\times$.

[40]The evolution of a laser pulse from noise is discussed by J. A. Fleck, Jr., Appl. Phys. Letters 13, 365 (1968).

[41]As pointed out in Sec. III B it is this relatively long phonon lifetime which enables us to obtain approximate analytical solutions for the avalanche burn out.

[42]We were not able to make any reliable determinations of the bottleneck constant σ by observing lattice relaxation in our samples. With the apparatus available it was not possible to obtain uniform initial excitation of the resonance line. Some preliminary tests showed that this deficiency would lead to major errors in the result.

[43]Considerable care was taken to ensure that the sampling fields H_1 were confined to a sufficiently narrow spectral region so that the trace was not distorted by averaging over tanh curves characterized by different values of α_t and $t_{1/2}$. The measurements were made in the center of the burn-out region, and tests were carried out to ensure that the result was not materially affected by any further narrowing of the sampling width.

[44]This is smaller than the gain constants which were estimated in Sec. II B. It is adopted here in an attempt to fit the initial portion of the avalanche curve. As we point out in the next paragraph, the avalanche curve is probably distorted by cross relaxation.

[45]It was found that $(1/M_z)(dM_z/dt)$ decayed exponentially with time in the range from 11 to 25 μsec as suggested by Eq. (4.5). Signal to noise was poor, however, and a fit could equally well have been made to other forms of decay function.

PHYSICAL REVIEW B VOLUME 3, NUMBER 7 1 APRIL 1971

Paramagnetic Resonance and Relaxation of Ce^{3+}, Nd^{3+}, Er^{3+}, and Yb^{3+} in PrF_3

F. J. Rachford and Chao-Yuan Huang
Department of Physics, Case Western Reserve University, Cleveland, Ohio 44106
(Received 4 November 1970)

The electron-paramagnetic-resonance spectra of 1% Ce^{3+}, 1% Yb^{3+}, 0.1% Er^{3+}, and 1% Nd^{3+} in PrF_3 were observed at 4.2 °K. The g factors are found to be $g_x=0.39\pm0.03$, $g_y=0.946\pm0.002$, $g_z=2.69\pm0.02$, $\theta=15.5°\pm0.5°$ for Ce^{3+}; $g_x=2.801\pm0.015$, $g_y=4.48\pm0.03$, $g_z=11.36\pm0.20$, $\theta=41.5°\pm1°$ for Er^{3+}; $g_x=3.47\pm0.03$, $g_y=5.427\pm0.03$, $g_z=1.205\pm0.01$, $\theta=9°\pm1°$ for Yb^{3+}; and $g_x=1.500\pm0.005$, $g_y=1.094\pm0.003$, $g_z=2.937\pm0.017$, $\theta=67°\pm2°$ for Nd^{3+}. The y axis is chosen in the plane perpendicular to the c axis. The other orthogonal axes show no clear relation to the crystal faces, the z axis being rotated θ degrees from the c axis. The hyperfine splitting due to Er^{167} of 47±3 G and due to Yb^{171} of 577±10 G were observed in the y-axis spectra. The spin-bath relaxation rates T_b^{-1} for these same trivalent rare earths PrF were observed in the temperature range $1.3<T<4.5$ °K at frequencies ~8.9 GHz. The Nd^{3+} data were fitted by $T_b^{-1}=2.85T+0.214\times10^{-2}T^9+0.378\times10^{11}e^{-61.5/T}$ (c axis); the Er^{3+} data by $T_b^{-1}=143T+0.125\times10^{10}e^{-56.4/T}$ (x axis showing a strong cross-relaxation first term; the Ce^{3+} data by $T_b^{-1}=0.753T+0.276\times10^{-3}T^9+0.171\times10^{11}e^{-78.3/T}$ (c axis) where an Orbach term $\propto e^{-95/T}$ may also be added, possibly indicating relaxation via the first excited level of Pr^{3+}; and the Yb^{3+} data by single terms proportional to T^2, which is probably due to cross relaxation to pairs.

I. INTRODUCTION

The availability and stable nonhydroscopic nature of the lanthanum trifluorides have lead to their study as possible maser materials. Consequently, electron-paramagnetic-resonance (EPR) and spin-relaxation experiments have determined the rhombic g-tensor components and relaxation mechanisms of trivalent rare-earth ions[1-4] substituted in crystals of LaF_3. Our work extends this investigation to PrF_3,[4] which, like LaF_3, has the tysonite crystal structure.

Three closely related crystal structures have been proposed for tysonite from the x-ray measurements.[5-10] All three are consistent with the Faraday-rotation experiments,[11,12] as interpreted by Van Vleck and Hebb,[10] but fail to account for the crystal-field symmetry observed at the lanthanide site by EPR spectrometry. Recent investigations of the Raman-active phonon modes[13,14] plus the previous EPR observations in LaF_3[1-3] have indicated convincingly that the homomorphic